Reg Environ Change
DOI 10.1007/s10113-012-0372-8

ORIGINAL ARTICLE

# Dynamic downscaling of the twentieth-century reanalysis over the southeastern United States

**V. Misra · S. M. DiNapoli · S. Bastola**

Received: 10 July 2012 / Accepted: 30 October 2012


**Abstract** A 108-year (1901–2008) downscaling of the twentieth-century reanalysis (20CR) using the Regional Spectral Model (RSM) has been conducted for the southeastern United States (SEUS) at a horizontal grid resolution of 10 km. This 108-year product, named as the Florida Climate Institute-Florida State University Land–Atmosphere Reanalysis for the southeastern United States at 10-km resolution version 1.0 [FLAReS1.0], has primarily been developed for anticipated application studies in hydrology, crop management, ecology, and other interdisciplinary fields in the SEUS. The analysis of this downscaled product reveals that it ameliorates the issue of artificial discontinuity in the precipitation time series of the 20CR from the variations inherent to RSM. This centennial scale product allows us to begin examining decadal scale variations of the regional features of the SEUS. The fidelity of the low-frequency variations of the winter rainfall associated with the Atlantic Multi-decadal Oscillation (AMO) and the Pacific Decadal Oscillation is reasonably well captured in FLAReS1.0. In fact, the modulation of the El Niño-Southern Oscillation (ENSO) teleconnection with the SEUS rainfall by AMO in the downscaled product is also validated with observations. The ENSO-associated variations of accumulated rainfall from landfalling hurricanes in the SEUS are also well simulated in the downscaled climate simulation. It is to be noted that the success of this dynamical downscaling is also because the global reanalysis of 20CR showed comparable fidelity in these low-frequency variations of the SEUS climate. This method of dynamic downscaling global reanalysis with inclusion of spectral nudging at large wavelengths (in this case $\geq$500 km) toward the driving global reanalysis (20CR) is sometimes referred as a form of regional reanalysis.

**Keywords** Atlantic multi-decadal oscillation · Hurricanes · Pacific Decadal Oscillation

## Introduction

There is a constant demand for high-resolution climate data that are reliable and easily accessible for conducting climate diagnostic analysis at local scales, or for understanding impacts of climate variations and change in hydrology, ecology, agricultural science, public health, and many other applied fields. In order to cater to this need in the southeastern United States (SEUS), we have dynamically downscaled the twentieth-century reanalysis version 2 (20CR; Compo et al. 2011) available at a horizontal resolution of approximately 200 km using the Regional Spectral Model (RSM; Kanamitsu et al. 2010) at 10-km resolution for 108 years from 1901 to 2008. The realism of the coastlines and the orography at 10 km of RSM in

**Electronic supplementary material** The online version of this article (doi:10.1007/s10113-012-0372-8) contains supplementary material, which is available to authorized users.

V. Misra (✉)
Department of Earth, Ocean and Atmospheric Science, Florida State University, P.O. Box 3064520, Tallahassee, FL 32306-4520, USA
e-mail: vmisra@fsu.edu

V. Misra · S. M. DiNapoli · S. Bastola
Center for Ocean-Atmospheric Prediction Studies, Florida State University, 2035 E. Paul Dirac Dr., 200 RM Johnson Bldg, Tallahassee, FL 32306-2840, USA

V. Misra
Florida Climate Institute, Florida State University, 2035 E. Paul Dirac Dr., 200 RM Johnson Bldg, Tallahassee, FL 32306-2840, USA

Published online: 15 November 2012

contrast to 200 km of 20CR over the SEUS is best illustrated in Fig. S1 (see supplementary material).

Dynamic downscaling of global reanalysis in some ways has been regarded as a form of regional reanalysis (von Storch et al. 2000). This analogy follows from the similarity in constraining the regional model with the global reanalysis at large wavelengths to using relatively coarsely spaced station observations to produce a gridded analysis at comparatively finer resolution in a data assimilation scheme. The regional climate simulations have improved significantly over the years especially ever since it was established that dynamic downscaling requires some form of nudging in the interior of the regional domain to reduce the large-scale drift of the regional climate model (von Storch et al. 2000; Castro et al. 2005; Kanamaru and Kanamitsu 2007; Kanamitsu et al. 2010). This paradigm for improving the fidelity of regional climate simulation is demonstrated quite well in our recent studies of dynamic downscaling over the SEUS (Misra et al. 2011; Stefanova et al. 2012) forced with global reanalysis of European Reanalysis (ERA40; Uppala et al. 2006) and National Centers for Environmental Prediction Reanalysis 2 (NCEPR2; Kanamitsu et al. 2002) at approximately 200-km grid resolution. In fact, Bastola and Misra (2012) show that the dynamically downscaled rainfall from global reanalysis is superior to statistically downscaled rainfall for hydrological simulations in many of the watersheds over the SEUS. However, despite its relative advantages and appropriateness to develop homogenous climate history, in a true sense dynamic downscaling of a coarse reanalysis falls short of a reanalysis in which observational data are assimilated.

The community at large, with growing understanding of low-frequency variations of climate such as El Niño and the Southern Oscillation (ENSO; Cane and Zebiak 1985; Philander 1990; Guilyardi et al. 2009, 2012), Atlantic Multi-decadal Oscillation (AMO; Kerr 2000; Enfield et al. 2001; Mingfang et al. 2009), and Pacific Decadal Oscillation (PDO; Mantua et al. 1997; Newman et al. 2003), which have periods that range from interannual to the decadal, is demanding high-resolution climate data to establish their impacts vis-à-vis global climate change impact. Given the large uncertainty in the regional climate projections from the global climate models used in the International Panel for Climate Change (IPCC) Assessment Report (AR4), downscaling the 20CR for over 100 years offers a very good opportunity to assess the relative roles of natural variations and climate change on regional- to local-scale climate. It should be noted that this study does not dwell on the future climate change impacts over the SEUS. The centennial downscaling of 20CR over the SEUS described in this paper is referred as the Florida Climate Institute-Florida State University Land–Atmosphere Reanalysis over the southeastern United States at 10-km resolution version 1.0 (FLAReS1.0). This paper in validating FLAReS1.0 also helps in describing the fidelity of the regional climate model to simulate the climate of the SEUS and its variations, as it is forced by potentially the best possible boundary forcing, viz., global reanalysis. In the next section we describe the datasets used in the study, followed by the presentation of our analysis of 20CR and FLAReS1.0 over the SEUS in Sect. 3 with final concluding remarks in Sect. 4.

## Dataset descriptions

The 20CR dataset follows from Compo et al. (2011). 20CR is a comprehensive global atmospheric circulation dataset spanning the period of 1871 to present, which is generated from assimilating only surface observations of synoptic mean sea-level pressure and using the UK Met Office HadISST (Rayner et al. 2003) monthly sea surface temperature and sea ice distributions as boundary conditions. 20CR uses the technique of ensemble Kalman filter for data assimilation (Whitaker and Hamill 2002) and is generated using 6-h forecasts from an experimental version of the National Centers for Environmental Prediction (NCEP) Atmospheric General Circulation Model (AGCM) as the first guess field. As is shown in Compo et al. (2011) and later in this paper, 20CR reproduces many of the global climate variations reasonably well, making it ideal for downscaling to glean impact on local- to regional-scale climate variations from it.

As mentioned earlier FLAReS1.0 was generated from downscaling an ensemble member of the 20CR using the RSM. The virtues of RSM, described in greater detail in Kanamaru and Kanamitsu (2007), Yoshimura et al. (2010), and Kanamitsu et al. (2010), are broadly that it is a well-tested model, which has been used in national intercomparison studies (Mearns et al. 2009), successfully adapted for climate studies at 10-km grid resolution in the SEUS (Misra et al. 2011; Stefanova et al. 2012). Kanamaru and Kanamitsu (2007) and Kanamitsu et al. (2010) show that RSM unlike other regional models is relatively insensitive to domain size and location of the lateral boundaries owing to its feature of Scale Selective Bias Correction (SSBC). The SSBC essentially nudges the rotational component of the wind of the RSM spectrally to the driving global reanalysis at specific wavelengths (in case of FLAReS1.0 $\geq$ 500 km), and the area average of the temperature perturbation over the regional domain is set to zero at every time step, thereby reducing the climate drift in the RSM significantly. FLAReS1.0 was generated in three streams with 5 years of overlap between streams to avoid any spin-up issues. The size of the domain of SEUS

(Fig. 1) is 226 × 148 grid points, with a time step of 30 s. The configuration of RSM in terms of its model physics is briefly outlined in Table 1. The data for most of the surface meteorological variables are stored at intervals of 1 h, while the whole atmosphere is stored at intervals of 3 h.

We validate the results from 20CR and FLAReS1.0 using Parameter-elevation Regressions on Independent Slopes Model (PRISM; Gibson et al. 2002). The PRISM data, which include monthly mean values of precipitation and minimum ($T_{min}$) and maximum ($T_{max}$) surface temperature for the downscaling period, are available at 4-km horizontal resolution. We also make use of National Centers for Environmental Prediction (NCEP) Climate Prediction Center (CPC) observed rainfall at 0.5°grid resolution for the period 1948–2008 (Higgins et al. 2000) at daily interval. This is the analysis of rain gauge-based rainfall estimates available for continental United States. This dataset is being used to verify the ENSO variations of rainfall accumulation from landfalling hurricanes in FLAReS1.0 and 20CR.

## Results

A comprehensive validation exercise of FLAReS1.0 is conducted in DiNapoli and Misra (2012), which included a discussion on the climatological bias, diurnal variations, and illustrations of specific weather extremes in FLAReS1.0. The study showed that FLAReS1.0 displayed a significant wet bias in southern Florida and in the

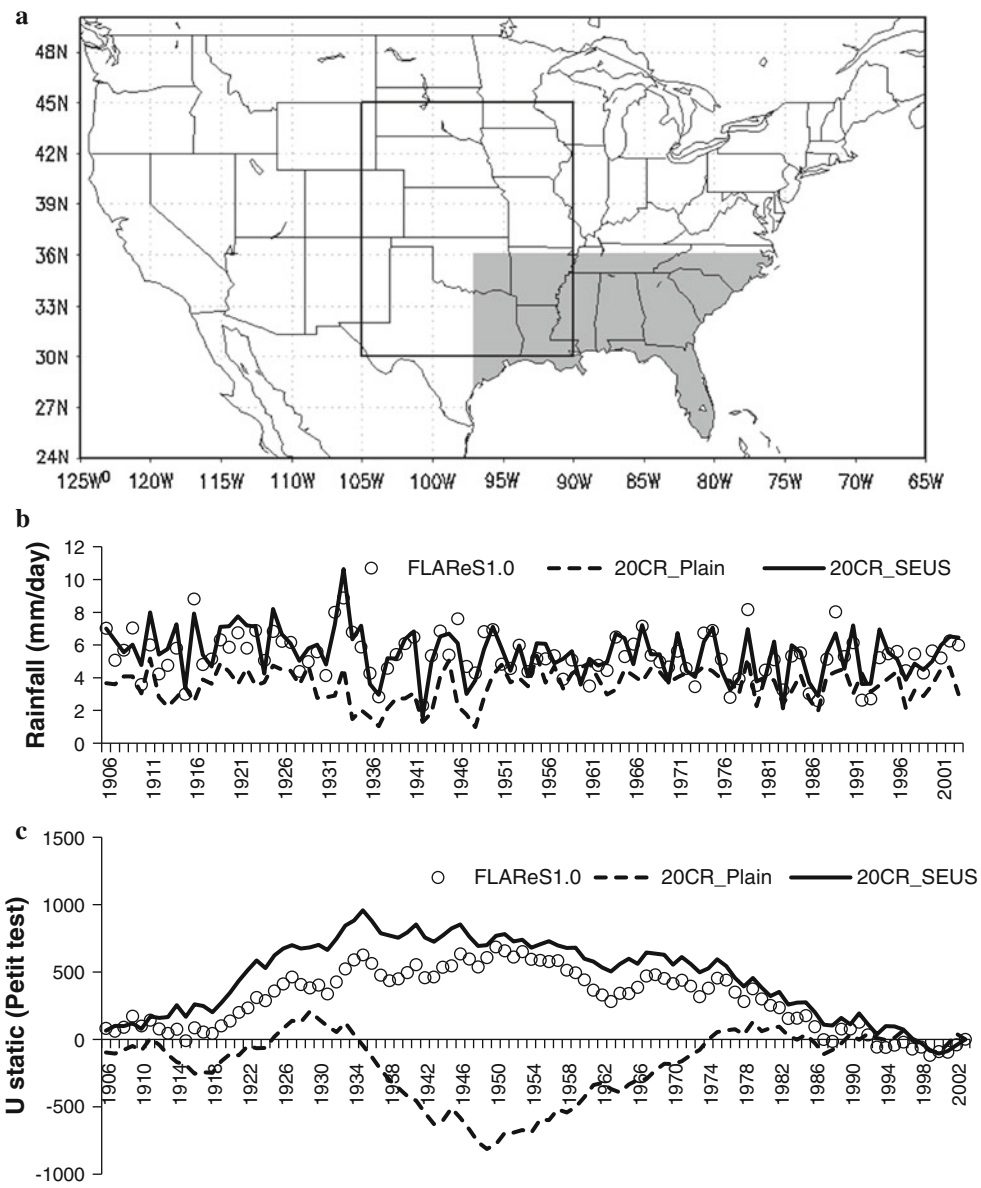


**Fig. 1** **a** The domain of the US central plains (*outlined*) and SEUS (*shaded*) over which the **b** the July monthly mean precipitation from 20CR and FLAReS1.0 is averaged. **c** The Pettitt test statistic for the three time series shown in (**b**) is plotted

**Table 1** Brief outline of RSM physics

| Boundary layer (nonlocal scheme) | Hong and Pan (1996) |
|---|---|
| Short-wave radiation | Chou et al. (1998) |
| Long-wave radiation | Chou and Suarez (1994) |
| Deep convection (simplified Arakawa-Schubert scheme) | Pan and Wu (1994) |
| Shallow convection | Tiedtke (1993) |
| Cloud parameterization | Slingo (1987) and updated as in Shimpo et al. (2008) |
| Land surface (NOAH) | Chen and Dudhia (2001) |

Carolinas that is accentuated in the boreal summer season. But this precipitation bias is systematic in FLAReS1.0 and can easily be corrected for its use in other application studies. The surface temperature bias in FLAReS1.0 on the other hand is within 1–2 °C (DiNapoli and Misra 2012). Furthermore, they show that the observed seasonal cycle of the surface temperature is nearly replicated by FLAReS1.0 in the majority of the SEUS region. In addition, DiNapoli and Misra (2012) show that several weather extremes like cold frontal passages, tropical cyclones, and sea breezes are well represented in FLAReS1.0. But they indicate that there is a systematic underestimation of the magnitude of most severe weather events. In this study we focus on detection of change points (or discontinuity) and decadal variations of the SEUS climate in FLAReS1.0 for surface temperature and precipitation.

## The data inhomogeneity issue in 20CR

Ferguson and Villarini (2012) found that 20CR suffers from an apparent discontinuity in the time series over the central plains of United States especially in the summer season due most likely to change in the density of synoptic observations of surface pressure. They observed that between 1940 and 1950 over the US central plains there was a steep increase in the density of observations assimilated in 20CR, which they said caused the apparent discontinuity in many of the meteorological variables. They therefore recommended that climate trend applications over US central plains be restricted to the later half-time period of the 20CR. But they recognized that this discontinuity in 20CR could vary regionally and seasonally. We examined for this discontinuity over the SEUS domain in both the 20CR and FLAReS1.0 monthly mean precipitation for July (as this was one of the variables used in Ferguson and Villarini 2012). We investigated for this discontinuity in the July monthly mean precipitation time series averaged over the SEUS domain of FLAReS1.0 (Fig. 1a) using the nonparametric Pettitt test for change point (Pettitt 1979; explained further in the supplementary material). The time series of the mean July precipitation from FLAReS1.0 and 20CR averaged over the SEUS is shown in Fig. 1b along with the 20CR monthly mean July precipitation time series from the US central plains for comparison. The corresponding Pettitt test statistic (U; see supplementary material) is plotted for all three time series in Fig. 1c. It is clearly seen from Fig. 1c and discussion in the supplementary material that the change point in 20CR July precipitation time series averaged over the US central plains (20CR_Plain) and over the SEUS (20CR_SEUS) is in 1949 and 1935, respectively. On the other hand, the corresponding time series in FLAReS1.0 (Fig. 1c) does not display any statistically significant change point. In other words, we suggest that the dynamic downscaling of 20CR over the SEUS in FLAReS1.0 makes the change point insignificant in relation to the internal variations inherent to FLAReS1.0.

## Teleconnection with the Pacific Decadal Oscillation

Figure 2a, b, and c shows the correlation of the January–February–March (JFM) rainfall variations over the SEUS with the PDO index in PRISM, 20CR, and FLAReS1.0 datasets. PDO index is defined as the first principal component of monthly sea surface temperature in the Pacific Ocean north of 20°N. PRISM observations (Fig. 2a) show correlation patterns that indicate wet (dry) anomalies over Florida and along the US Gulf coast (northern Alabama, Georgia, and Arkansas) during the positive (negative) phase of PDO, which is similar to the ENSO teleconnection over the region. In fact, Gershunov and Barnett (1998) suggested that PDO augments the ENSO teleconnection over the continental United Stated as in Fig. 2a. 20CR captures this teleconnection of the SEUS winter rainfall with the PDO (Fig. 2b) reasonably well in comparison with the PRISM observations (Fig. 2a). This teleconnection is also reproduced by FLAReS1.0 (Fig. 2c), which reflects the usability of this relatively high-resolution dataset for other application studies to study the impact of the low-frequency variations associated with PDO. It is argued that the ability of the FLAReS1.0 to preserve these low-frequency teleconnections from 20CR is in itself a virtue of the regional climate simulation. In effect FLAReS1.0 is able to provide a dynamically and physically consistent set of meteorological variables at 10-km grid resolution that seems to obey the large-scale climate variations.

## Teleconnection with the Atlantic multi-decadal oscillation

Similarly, Fig. 3 shows the teleconnection of the JFM rainfall over the SEUS with the ENSO index during positive and negative phases of the AMO. Consistent with the

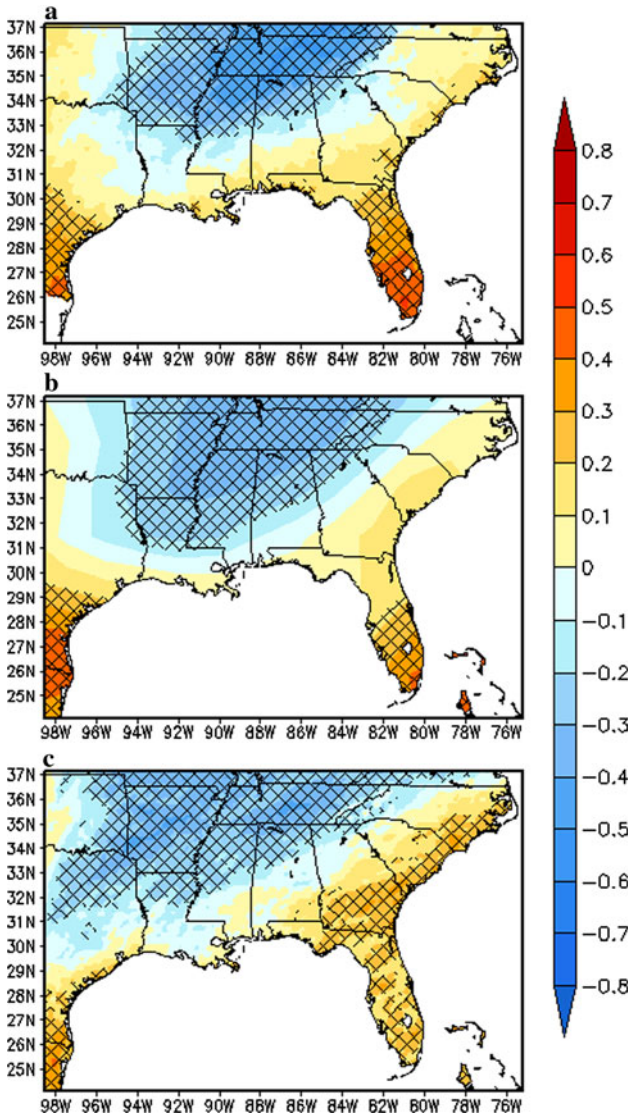


**Fig. 2** The correlation of the Pacific Decadal Oscillation (PDO) index with the mean January–February–March rainfall from **a** PRISM, **b** 20CR, and **c** FLAReS1.0. Correlations at the 95 % confidence interval according to *t* test are hashed

previous studies (Mo 2010; Enfield et al. 2001), the ENSO teleconnection with the SEUS shows variability with the AMO phase in observations (Fig. 3a, b), in 20CR (Fig. 3c, d), and in FLAReS1.0 (Fig. 3e, f). A positive phase of AMO (in Fig. 3a, c, e) entails that warm ENSO events are associated with wet (dry) winter anomalies confined largely over peninsular Florida (spread from Louisiana northeastward to Tennessee). On the other hand, the negative phase of AMO (Fig. 3b, d, f) entails that the warm ENSO events are associated with wet (dry) winter anomalies over a widespread region along the US Gulf coast to the coasts of the Carolinas (confined largely over Tennessee). It should be noted that the reproduction of this observed teleconnection in 20CR and in FLAReS1.0 is quite remarkable.

## ENSO variations of landfalling hurricanes in the SEUS

Several studies have pointed to the influence of ENSO on landfalling hurricanes in the United States and in the Caribbean region (Richards and O'Brien 1996; Bove et al. 1998; Tartaglione et al. 2003; Smith et al. 2007). These studies show in general that in El Niño years the landfalling hurricanes are far less than in neutral or La Niña years. For example, Bove et al. (1998), using nearly 100 years of observed data, indicate that the probability of two or more hurricanes making a landfall is 23 % in warm ENSO years as opposed to 58 % in neutral phase and 63 % in cold ENSO years. This effect from ENSO is largely through the modulation of the vertical shear across the tropical Atlantic (Gray 1984). In Fig. 4 we show the accumulated rainfall of all hurricanes in the period 1948–2000 that have made landfall in the SEUS domain of FLAReS1.0 from 20CR, FLAReS1.0, and NCEP CPC daily rainfall, with nine (24) landfalling hurricanes used for El Niño (La Niña) years in the composite. We used the period from 1948 onward as the observed daily NCEP CPC rainfall was only available since then. To prepare this figure, we began accumulating the rainfall from the date that the center of the hurricane moved inland (using the U.S. National Hurricane Center best track data) until one of the following conditions was met:

1. The center moved back over water;
2. The center moved out of the FLAReS1.0 domain;
3. The National Hurricane Center stopped issuing advisories (either due to the hurricane's dissipation or its extratropical transition).

The statistical 90 % confidence level of these composites was determined by applying the bootstrapping technique (McClave and Dietrich 1994; Efron and Tibshirani 1993). The significance test on the observed rainfall composites in La Niña year composites (Fig. 4b) indicates that they are largely statistically significant. In contrast, in El Niño years the relative minimum along the western part of the domain in El Niño years (Fig. 4a) appears to be the only region that is statistically significant. The results of these observed composites are consistent with the observational study of Klotzbach (2011) which notes that the reduction in landfalling hurricanes along the east coast is greater than along the Gulf coast in El Niño years. However, the regions with large rainfall accumulation from these landfalling hurricanes are off center of the hurricane as the spiral rainbands around the eye of the hurricane contribute significantly to the rainfall amounts. It is quite noteworthy that despite the coarse resolution of 20CR, it is

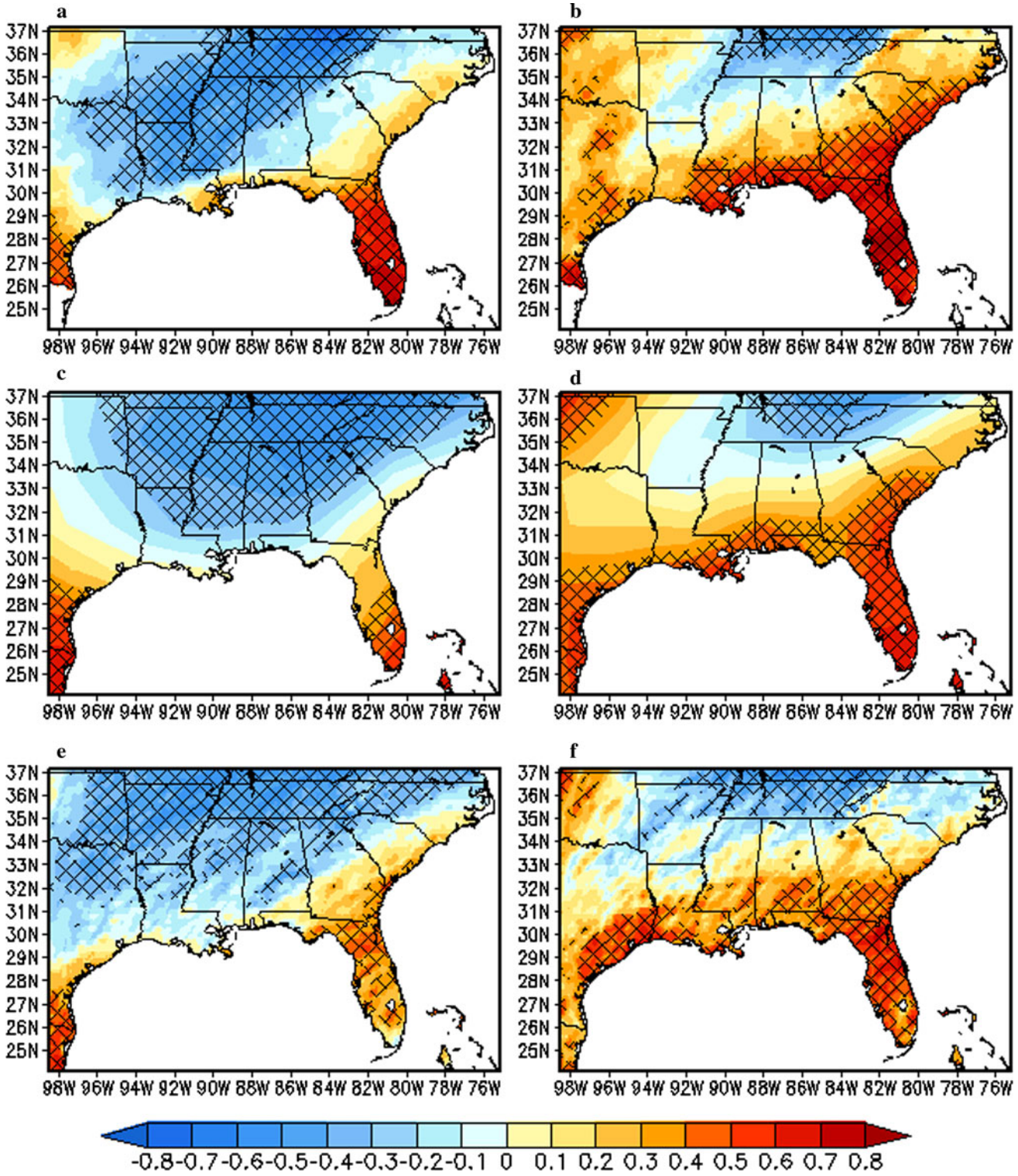


**Fig. 3** The correlation of the ENSO index (see text) with JFM rainfall from PRISM during **a** positive (1930–1959) and **b** negative phase (1965–1989) of the AMO index (see text). Similarly, the correlation of the ENSO index with JFM rainfall from **c** 20CR and **e** FLAReS10 during positive and **d** 20CR and **f** FLAReS1.0 during negative phase of the AMO index is shown

able to replicate this interannual feature of the landfalling hurricanes remarkably well (Fig. 4c, d). It is able to pick the maximum along the Carolina coasts and relative minimum in south Florida during La Niña years (Fig. 4d). Similarly, the gradient of rainfall in the western part of the domain is also depicted well in 20CR in El Niño years

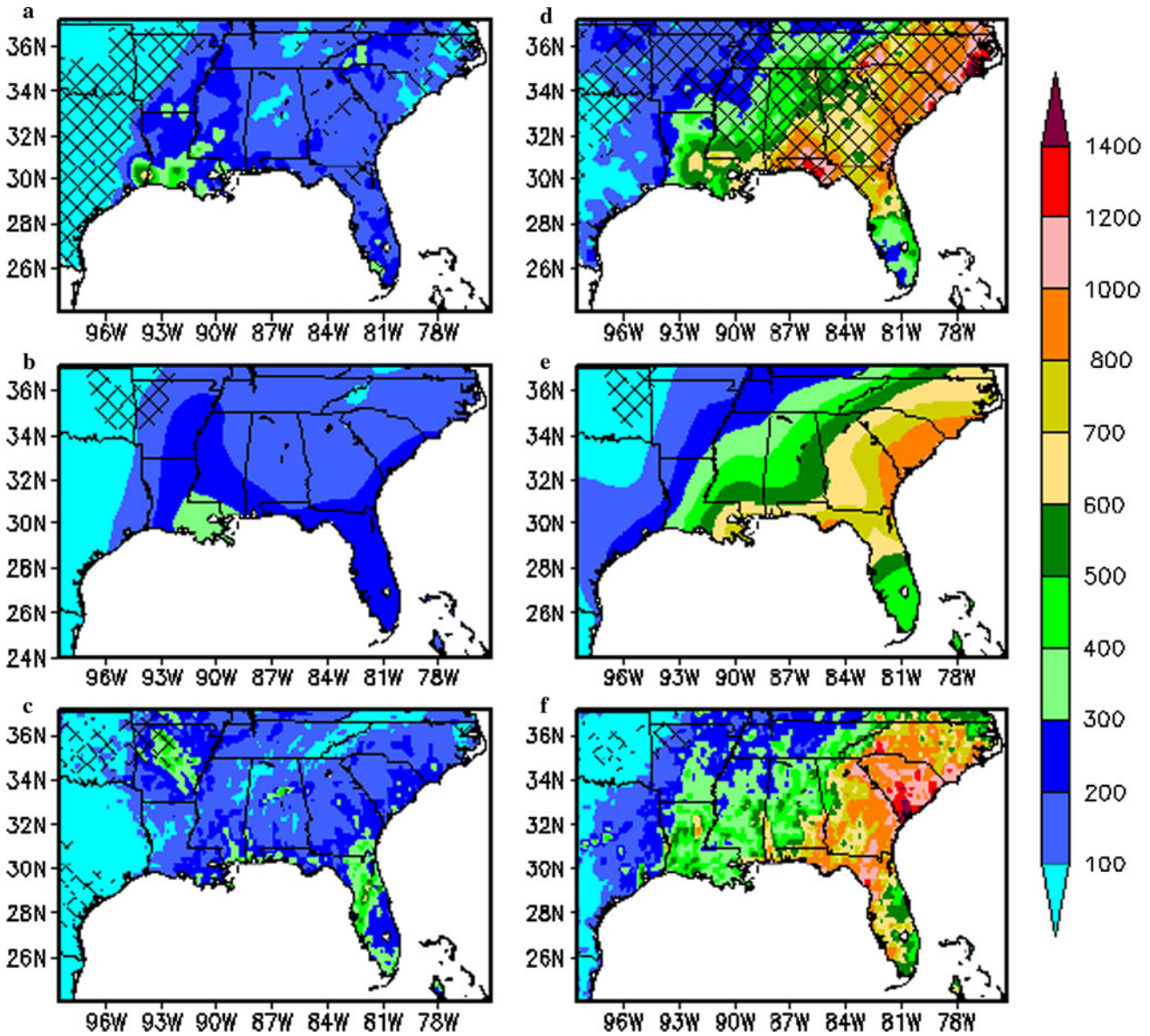


**Fig. 4** The composite of rainfall for El Niño years for all landfalling hurricanes in the SEUS between 1948 and 2000 from **a** NOAA CPC, **b** 20CR, and **c** FLAReS1.0 rainfall. **d**, **e,** and **f** are same as (**a**), (**b**), and (**c**) but for La Niña years. The units are in millimeters. The hashes are depicting statistical significance at 10 % significance level from bootstrapping a 1,000 times

(Fig. 4c). FLAReS1.0 is able to closely follow the features displayed by 20CR (Fig. 4e, f). It could be argued that FLAReS1.0 deteriorates some of the features like with erroneous maximum rainfall appearing in central Florida and Arkansas in El Niño years (Fig. 4e) or the higher than observed rainfall in south Florida in La Niña years (Fig. 4f). However, it should be noted that FLAReS1.0 is able to pick the gradients of rainfall and the higher maximum along the panhandle Gulf coast of Florida and Atlantic coasts of the Carolina's far better than the 20CR (Fig. 4f). However, the location of maximum rainfall over the coast of South Carolina (Fig. 4f) is unsupported by observations (Fig. 4b). Furthermore, it may be noted that at the 2° grid resolution of the 20CR, most of peninsular south Florida is unresolved as land (see supplementary material) and therefore, the gradients of rainfall from landfalling hurricanes are a bit unreliable even though it happens to match the observations quite well.

## Discussion and conclusions

In this study we have downscaled the twentieth-century global reanalysis (20CR) to 10-km grid resolution using the Regional Spectral Model (Kanamitsu et al. 2010) over the Southeastern United States (SEUS). This exercise was

primarily motivated from the demand for such spatial resolution of surface meteorology data for many application studies in the region including hydrology, ecology, and crop modeling. This paper shows that the dynamic downscaling of 20CR reduces the artificial discontinuity of the precipitation. Furthermore, FLAReS1.0 has reliably reproduced the dominant low-frequency variations in the winter climate of the SEUS associated with the AMO, the PDO, and the ENSO, which raises the confidence in using the data for other application studies. The SEUS region has one of the strongest influences of ENSO in the continental United States, especially in the winter time, which, however, seems to get modulated by AMO. This is also well simulated in the FLAReS1.0. The fidelity of the 20CR both in the low-frequency variability of the winter climate and that in the landfalling hurricanes in the summer and fall seasons in the SEUS is commendable. It makes dynamic downscaling of 20CR all the more relevant. It could be argued that FLAReS1.0 does display a deterioration of these teleconnections especially over south Florida relative to 20CR (Figs. 2, 3). But given the erroneous coastlines from the coarse resolution of 20CR (Fig. S1) which depicts a large fraction of the south Florida land region as ocean makes the fidelity of such teleconnections in 20CR questionable.

It may be noted that FLAReS1.0 and 20CR verify with observations most reasonably in the boreal winter season. This is not surprising given its strong teleconnection with large-scale variations of SST (e.g., ENSO, AMO, and PDO) in this season. In the other seasons of the year, such strong teleconnections are weaker. However, diurnal variations are quite prominent in the transition (spring and fall) and summer seasons. DiNapoli and Misra (2012) have shown that FLAReS1.0 also simulates the diurnal variations in the summer season reasonably well, which adds to the value of using the output from FLAReS1.0 for other application studies. FLAReS1.0 by the same token could also serve as a high spatial and temporal resolution validation dataset for verifying downscaled data from global climate models for the current climate, especially for verifying the low-frequency variations that require multi-decadal time periods.

A data assimilation approach to generate regional reanalysis may be desirable as an alternative to FLAReS1.0. However, lack of observations especially in the earlier decades of the twentieth century and nonuniformity of both the coverage and type of observation over such a long period of over 100 years could make such a regional reanalysis inappropriate for climate diagnostics. On the other hand, given the reasonable fidelity and the relative ease with which FLAReS1.0 was generated would make such century-long downscaling from global reanalysis an attractive option to broaden the application of climate datasets in other fields. The fact that FLAReS1.0 is able to preserve the observed teleconnections of the SEUS climate and provide dynamically consistent meteorological variables at significantly higher temporal and spatial resolutions is in itself an added value to 20CR.

**Acknowledgments** This work was supported by grants from NOAA (NA07OAR4310221), USGS (06HQGR0125), and USDA (027865). Its contents are solely the responsibility of the authors and do not necessarily represent the official views of the acknowledged funding agencies.

## References

Bastola S, Misra V (2012) Evaluation of dynamically downscaled reanalysis precipitation data for hydrological application of watersheds in the southeast United States. Hydrol Process. Submitted

Bove MC, Elsner JB, Landsea CW, Niu X, O'Brien JJ (1998) Effects of El Niño on US landfalling hurricanes, revisited. Bull. Am Meteor Soc 79:2477–2482

Cane MA, Zebiak SE (1985) A theory for El Niño and the Southern Oscillation. Science 228:1085–1087

Castro CL, Pielke RA Sr, Leoncini G (2005) Dynamical downscaling: assessment of value retained and added using the regional atmospheric modeling system (RAMS). J Geophys Res 110:D05108. doi:10.1029/2004JD004721

Chen F, Dudhia J (2001) Coupling an advanced land-surface hydrology model with the Penn State/NCAR MM5 modeling system. Part I: model implementation and sensitivity. Mon Wea Rev 129:569–585

Chou MD, Suarez MJ (1994) An efficient thermal infrared radiation parameterization for use in general circulation models. Technical report series on global modeling and data assimilation, NASA/TM-1994-104606, 3, 85 pp

Chou M-D, Suarez MJ, Ho C-H, Yan MM-J, Lee K-T (1998) Parameterizations for cloud overlapping and shortwave single-scattering properties for use in general circulation and cloud ensemble models. J Climate 11:202–214

Compo GP et al (2011) The twentieth century reanalysis project. Q J R Meteorol Soc 137:1–28

DiNapoli S, Misra V (2012) Reconstructing the 20th century high-resolution climate of the Southeastern United States. J Geophys Res (Atmospheres) 117:D19113. doi:10.1029/2012JD018303

Efron B, Tibshirani RJ (1993) An introduction to the bootstrap. Chapman and Hall, London

Enfield DB, Mestaz-Nunez AM, Trimble PJ (2001) The Atlantic multidecadal oscillation and its relation to rainfall and river flows in the continental US. Geophys Res Lett 28:2077–2080

Ferguson CR, Villarini G (2012) Detecting inhomogeneities in the twentieth century reanalysis over the central United States. J Geophys Res 117:D05123. doi:10.1029/2011JD016988

Gershunov A, Barnett TP (1998) Interdecadal modulation of ENSO teleconnections. Bull Am Meteorol Soc 80:2715–2725

Gibson W et al (2002) Development of a 103-year high-resolution climate data set for the conterminous United States. In: Proceedings of 13th American meteorological society conference on applied climatology, Portland, OR, pp 181–183

Gray WM (1984) Atlantic seasonal hurricane frequency. Part I:El Niño and 30 mb quasi-biennial oscillation influences. Mon Wea Rev 112:1649–1668

Guilyardi E, Wittenberg A, Fedorov A, Collins M, Wang C, Capotondi A, von Oldengorgh GJ, Stockdale T (2009)

Understanding El Niño in ocean–atmosphere general circulation models: progress and challenges. Bull Am Meteorol Soc 90:325–340

Guilyardi E, Cai W, Collins M, Fedorov A, Jin F-F, Kumar A, Sun D-Z, Wittenberg A (2012) New strategies for evaluating ENSO processes in climate models. Bull Am Meteorol Soc 93:235–238

Higgins RW, Shi W, Yarosh E, Joyce R (2000) Improved United States precipitation quality control system and analysis. NCEP/CPC ATLAS No. 7. Also available at: http://www.cpc.ncep.noaa.gov/research_papers/ncep_cpc_atlas/7/index.html

Hong S-Y, Pan H-L (1996) Nonlocal boundary layer vertical diffusion in a medium-range forecast model. Mon Wea Rev 124:2322–2339

Kanamaru H, Kanamitsu M (2007) Scale-selective bias correction in a downscaling of global analysis using a regional model. Mon Wea Rev 135:334–350

Kanamitsu M, Ebisuzaki W, Woollen J, Yang S-K, Hnilo JJ, Fiorino M, Potter GL (2002) NCEP-DOE AMIP-II reanalysis (R-2). Bull Am Meteor Soc 83:1631–1643

Kanamitsu M, Yoshimura K, Yhang Y-B, Hong S-Y (2010) Errors of interannual variability and multi-decadal trend in dynamical regional climate downscaling and its corrections. J Geophys Res 115:D17115. doi:10.1029/2009JD013511

Kerr RA (2000) A North Atlantic climate pacemaker for the centuries. Science 288:1984–1986

Klotzbach PJ (2011) El Niño-southern oscillation's impact on Atlantic Basin Hurricanes and US. Landfalls J Climate 24:1252–1263

Mantua NJ, Hare SR, Zhang Y, Wallace JM, Francis R (1997) A Pacific interdecadal climate oscillation with impacts on salmon production. Bull Am Meteorol Soc 78:1069–1079

McClave JT, Dietrich FH II (1994) Statistics. MacMillan College Publishing Co, New York

Mearns LO, Gutowski WJ, Jones R, Leung L-Y, McGinnis S, Nunes AMB, Qian Y (2009) A regional climate change assessment program for North America. EOS Trans. 90:311–312

Mingfang T, Kushnir Y, Seager R, Li C (2009) Forced and internal twentieth-century SST trends in the North Atlantic. J Climate 22:1469–1481. doi:10.1175/2008JCLI2561.1

Misra V, Moeller L, Stefanova L, Chan S, O'Brien JJ, Smith III TJ, Plant N (2011) The influence of the Atlantic Warm Pool on the Florida panhandle sea breeze. J Geophys Res 116:D00Q06. doi:10.1029/2010JD015367

Mo KC (2010) Interdecadal modulation of the impact of ENSO on precipitation and temperature over the United States. J Climate 23:3639–3656

Newman M, Compo GP, Alexander MA (2003) ENSO-forced variability of the Pacific decadal oscillation. J Climate 16:3853–3857

Pan H-L, Wu W-S (1994) Implementing a mass-flux convective parameterization package for the NMC medium range forecast model. Preprints, 10th conference on numerical weather prediction, Portland, OR, American Meteorological Society, pp 96–98

Pettitt AN (1979) A non-parametric approach to the change-point problem. Appl Stat 28:126–135. doi:10.2307/2346729

Philander SG (1990) El Niño, La Niña, and the Southern Oscillation. Academic Press, San Diego, CA

Rayner NA, Parker DE, Horton EB, Folland CK, Alexander LV, Rowell DP, Kent EC, Kaplan A (2003) Global analysis of sea surface temperature, sea ice, and night marine air temperature since the late nineteenth century. J Geophys Res 108:4407. doi:10.1029/2002JD002670

Richards TS, O'Brien JJ (1996) The effect of El Niño on US landfalling hurricanes. Bull Am Meteor Soc 77:773–774

Shimpo A, Kanamitsu M, Iacobellis SF, Hong S-Y (2008) Comparison of four cloud schemes in simulating the seasonal mean field forced by the observed sea surface temperature. Mon Wea Rev 136:2557–2575

Slingo JM (1987) The development and verification of a cloud prediction scheme for the ECMWF model. Q J R Meteorol Soc 113:899–927

Smith SR, Brolley J, O'Brien JJ, Tartaglione CA (2007) ENSO's impact on regional US hurricane activity. J Climate 20:1404–1414

Stefanova L, Misra V, Chan S, O'Brien JJ, Smith TJ III (2012) A proxy for high resolution regional reanalysis for the Southeast United States: assessment of precipitation variability. Climate Dyn 38:2449–2466

Tartaglione CA, Smith SR, O'Brien JJ (2003) ENSO impact on hurricane landfall probabilities for the Caribbean. J Climate 16:2925–2931

Tiedtke M (1993) Representation of clouds in large-scale models. Mon Wea Rev 121:3040–3061

von Storch H, Langenberg H, Feser F (2000) A spectral nudging technique for dynamic downscaling purposes. Mon Wea Rev 128:3664–3673

Uppala SM et al (2006) The ERA40 re-analysis. Q J R Meteorol Soc. doi:10.1256/qj.04.176

Whitaker JS, Hamill TM (2002) Ensemble data assimilation without perturbed observations. Mon Wea Rev 130:1913–1924

Yoshimura K, Kanamitsu M, Dettinger M (2010) Regional downscaling for stable water isotopes: a case study of an atmospheric river event. J Geophys Res 115:D18114

# Supplementary material

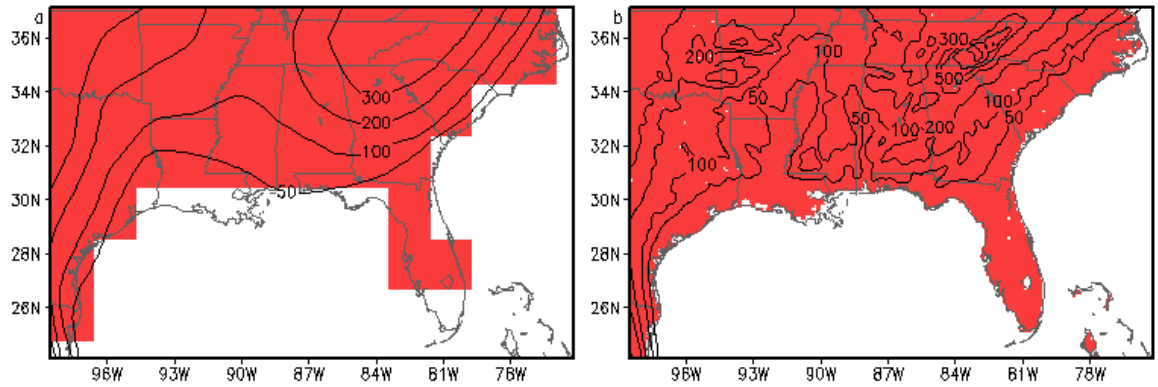


Figure S1: The land/ocean mask with land shaded in red overlaid with surface geopotential height (contoured) in meters at a) 20CR resolution of 200km and at b) FLAReS1.0 resolution of 10km.

**The Pettitt test**

The pettitt test is a non-parametric test for detecting change points in time series. It is given by equations 1 and 2 (Pettitt 1979) given below:

$$U_k = 2\sum_{i=1}^{k} R_i - k(N+1) \quad \text{for k} = 1.,.,.,\text{N} \qquad (1)$$

$$U = \max|U_k| \qquad (2)$$

$$p = 1 - \exp(-6U^2/(N^3 + N^2)) \qquad (3)$$

Where R is the rank of i*th* observation; N is the number of time steps, $U_k$, is the test statistic for k*th* year. The change point is located at a time step where the absolute value of the test statistic is maximum. We then use equation (3) above in order to test the statistical significance for the probability of a change point i.e., the point with largest value of the test statistic U (Pettitt (1979).

The time series will continuously increase or decrease in the absence of any change point. However the test statistic will increase (decrease) up to the change point and then decrease (increase) if there is any discontinuity in the timeseries. The maximum value of the U statistic occurred in 1950, 1949 and 1935 for FLAReS1.0, 20CR_SEUS and 20CR_Plain respectively. The probability associated with concluding these as potential change points (Equation 3) is 0.948, 0.99 and 0.996 for FLAReS1.0, 20CR_Plain and 20CR_SEUS respectively. This clearly shows that the potential change point in FLAReS1.0 is statistically insignificant at 5% (0.95) and even at 1% (0.99) significance level. On the other hand the change point for 20CR_SEUS and 20CR_Plain is statistically significant at the 1% and even at 5% significance levels. It should be mentioned that at the time of the change point of 20CR_SEUS (1935), the rainfall in the FLAReS1.0 displays far less of a magnitude of the U parameter (Fig. 1c).

The point for showing 20CR_Plain was to reproduce the result of Ferguson and Villarini (2012) in validation of the Pettitt test to detect change points. Furthermore, they argued that the discontinuity in 20CR_Plain in 1949 was associated with abrupt change in the density of surface observations over the central plains. However they acknowledge that this period of abrupt change in data density can change from region to region and time of the year.